

SPECTROSCOPY AND PHOTOPHYSICS OF 3'-[*p*-(DIMETHYLAMINO)PHENYL]SPIRO- [FLUORENE-9, 4'-OXAZOLIDINE]-2', 5'-DIONE

J. DOBKOWSKI, R. KOŁOS AND J. WALUK

Institute of Physical Chemistry, Polish Academy of Sciences
Kasprzaka 44/52, Warszawa, Poland

(Received April 14, 1995; revised version June 8, 1995;
in final form June 28, 1995)

*Dedicated to Professor Zdzisław Ruziewicz on the occasion of his 70th birthday**

Electronic absorption and emission spectroscopy of the title molecule has been studied in solution, low-temperature glasses and polymer matrices. No luminescence could be observed down to 77 K. In the presence of water, the formation of the hydrated species was observed, accompanied by the appearance of phosphorescence. The structure and spectra of both forms were calculated using molecular mechanics and quantum chemical methods. The lack of phosphorescence in the anhydride is interpreted as due to proximity effects in the triplet manifold.

PACS numbers: 33.10.-n

1. Introduction

Molecules with close-lying $\pi\pi^*$ and $n\pi^*$ electronic transitions often exhibit quite unusual photophysics. Vibronic interaction between the two types of states, termed proximity effects [1], may account for such phenomena as strong variations of luminescence yields with the hydrogen bonding properties of the solvent, solvent and temperature-dependent triplet yields, or deuterium isotope effects whose magnitude changes with the position of substitution. Many azaheterocyclic and aromatic carbonyl compounds provide examples of such pseudo Jahn-Teller interaction. For instance, phosphorescence of cinnoline [2], phthalazine [3] and 9,10-diazaphenanthrene [4] is only observed in protic solvents. In benzo[f]quinoxaline, phosphorescence is extremely weak in frozen hydrocarbons, but much more intense in hydroxylic glasses [5].

*Submitted on invitation of the Institute of Physical and Theoretical Chemistry, Technical University of Wrocław, Wrocław, Poland.

The planar symmetry of most heteroaromatic systems dictates that the interaction between $\pi\pi^*$ and $n\pi^*$ states occurs via the vibronically active out of plane bending modes. Their appearance in the spectra is often considered as manifestation of proximity effects [5].

In this paper, we study 3'-[*p*-(dimethylamino)phenyl]spiro-[fluorene-9,4'-oxazolidine]-2',5'-dione (DFOD), a molecule exploited as an attractive candidate for the use in UV-dosimetric applications [6]. It has orbitals of local π or n character, but the lack of overall symmetry leaves no restrictions with respect to the interaction of states and the allowed transition moment directions. This leads to interesting spectral and photophysical consequences: (i) lack of emission in DFOD; (ii) inducing the phosphorescence in the hydrated form by the "chemical removal" of proximity effects; (iii) depolarization of phosphorescence.

2. Experimental

3'-[*p*-(dimethylamino)-phenyl]spiro-[fluorene-9,4'-oxazolidine]-2',5'-dione was kindly supplied by Chemipan, Warsaw. Butyronitrile (BuCN) was repeatedly distilled over CaCl_2 and P_2O_5 , water-quadruply distilled in quartz vessels. Other solvents (Merck, spectral grade) were used without further purification.

The room and low temperature absorption spectra were recorded by means of a Shimadzu UV 3100 spectrometer. The luminescence and excitation spectra were recorded with a Jasny spectrofluorimeter [7] equipped with a photon counting detection system.

Linear dichroism curves were measured in stretched poly(vinyl alcohol) (PVA) sheets (Sigma, mol. weight 70000–100000) and analyzed using the TEM procedure [8].

3. Results

Room temperature absorption spectra of DFOD were recorded in protic and aprotic solvents characterized by different polarity (Fig. 1).

The shape and the spectral position of the bands in the absorption spectrum are independent of the solvent, with the exception of water, where a blue shift of the most intense band has been observed. In an attempt to get a better understanding of this spectral shift we have studied the absorption spectra of DFOD in several mixed solvents: (I) methanol/ H_2O (1:4 v/v), (II) methanol/ H_2O , (III) *n*-propanol/ H_2O , (IV) BuCN/ H_2O ; the water content was *ca.* 0.05% in II and III and 0.3% in IV, respectively. The absorption spectra of DFOD recorded as a function of time in (II) exhibited significant evolution with well defined isosbestic points (Fig. 2). Similar effect was observed in the case of solvent (I); however, in *n*-propanol the process was much slower. We attribute the spectral changes to the formation of a hydrated form of DFOD. Contrary to the results in the alcohol/water mixtures, the absorption spectrum of DFOD in (IV) did not show any evolution.

No luminescence could be detected at room temperature in any solvent in the range 600–350 nm. At low temperature (77 K) the phosphorescence was observed in (I) (Fig. 3) as well as in (III). In BuCN and 2-methylbutane the emission

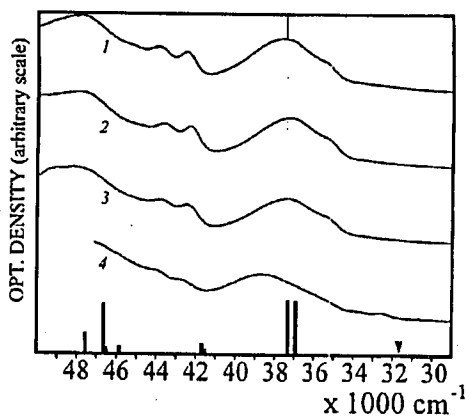


Fig. 1. Room temperature absorption spectra of DFOD in 2-methylbutane (1), butyronitrile (2), *n*-propanol (3) and in water (4). The bars indicate the calculated transitions for which the oscillator strength is higher than 0.05 (see Table I). The triangle shows the computed position of the lowest excited singlet state.

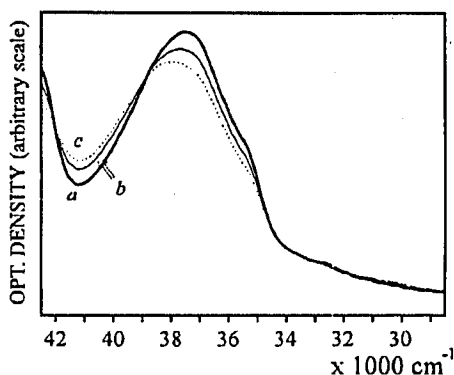


Fig. 2. Room temperature absorption spectra of DFOD in MeOH (water content *ca.* 0.05% v/v) recorded as a function of time; *a* — fresh solution, *b* — 1h after preparation, *c* — 4 h after preparation.

was undetectable. The phosphorescence excitation spectrum in (I) reproduces well the low temperature absorption (Fig. 3) which, in turn, coincides with the room temperature absorption of the hydrated form. The same phosphorescence was also observed in the PVA sheet, which was cast from the water solution and, naturally, contained the hydrate.

We thus conclude that DFOD is non-luminescent even at 77 K. The observed phosphorescence is assigned to the hydrated form.

The values of the phosphorescence anisotropy as well as those of the anisotropy of phosphorescence excitation are close to zero (Fig. 3). The trivial reasons of depolarization may be rejected: the optical quality of the sample was checked dur-

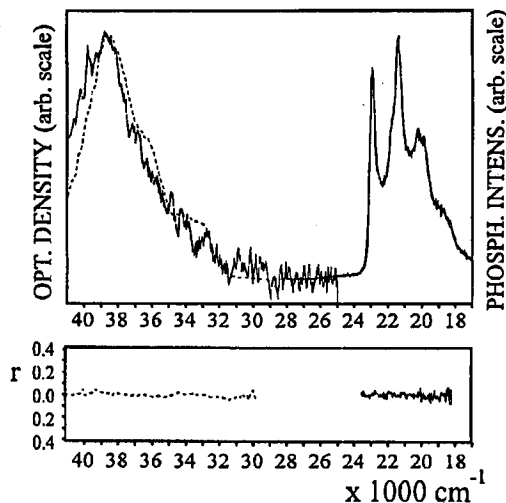


Fig. 3. Normalized low temperature (77 K) spectra of DFOD in MeOH/H₂O (1:4 v/v). Upper panel: phosphorescence and absorption (solid line), phosphorescence excitation (dashed line). Lower panel: phosphorescence anisotropy (solid line) and phosphorescence excitation anisotropy (dashed line).

ing the measurement, and the low solute concentration precluded efficient energy transfer.

4. Molecular mechanics and quantum chemical calculations

Ground state structures of DFOD and its hydrated form calculated using the MMX force field [9] are presented in Fig. 4. It should be noted that the DFOD molecule does not assume the highest possible symmetry, C_s , which would correspond to the coplanarity of the diaminophenyl group and the dione skeleton: the angle between the two planes is calculated to be 22°.

Calculations of singlet and triplet excitation energies, oscillator strengths, transition moment directions and charge density distributions were performed using the INDO/S method, separately parametrized for singlet [10] and triplet [11] states. 200 lowest singly excited configurations were taken into account in the CI procedure. The results are presented in Tables I–IV. Figs. 5 and 6 show the highest filled and the lowest unoccupied orbitals which contribute the most to the low-lying transitions.

For the singlet manifold of DFOD (Table I) it is predicted that the lowest excited state is very weakly allowed and corresponds to an excitation from the lone pair orbitals on the carbonyl oxygen atoms into the fluorene π^* orbital. Four next states correspond to transitions localized either on the fluorene or on the dimethylaniline moieties: these may be called "local" $\pi\pi^*$ states. The localization of excitation is a consequence of the shape of the molecular orbitals which contribute to a transition. Visual inspection (Fig. 5) shows that some orbitals are restricted to either the fluorene or the dimethylaniline part. Quantitatively, the de-

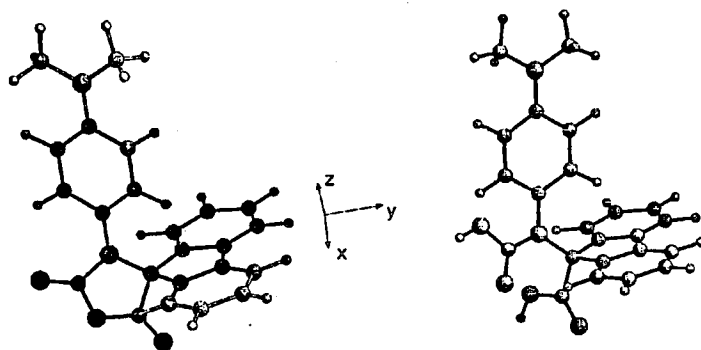


Fig. 4. The geometry of DFOD (left) and its hydrate (right) optimized by MMX. The x and y axes lie in the fluorene plane.

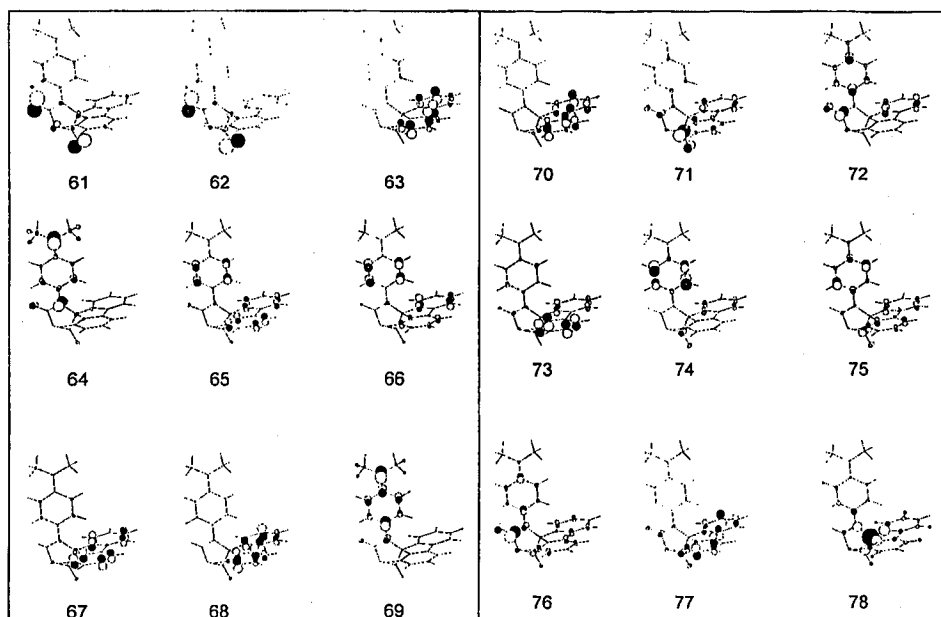


Fig. 5. Highest occupied molecular orbitals (left panel) and lowest unoccupied molecular orbitals (right panel) of DFOD relevant for the low energy transitions (see Tables I and II).

gree of localization, DL , of an orbital ψ_k on a certain part of a molecule (denoted by A), is given by

$$DL^A(\psi_k) = \sum_i^{N_A} c_{ik}^2,$$

TABLE I

Singlet transitions of DFOD calculated by INDO/S. In bold, the transitions discussed in text.

	En. ^a	<i>f</i>	<i>M_x</i>	<i>M_y</i>	<i>M_z</i>	α^b [deg]	DM ^c [D]	Leading configurations ^d
1	31.66	0.003	-0.37	0.18	0.10	0	6.46	0.57(62-71)-0.46(61-71)
2	33.30	0.032	-0.37	1.39	0.03	50	7.77	0.70(69-74)+0.41(69-75)
3	34.22	0.003	-0.05	0.43	-0.04	60	7.47	0.57(67-70)+0.50(68-71)
4	34.81	0.030	-1.29	0.05	0.40	23	6.65	0.47(68-73)
5	34.85	0.031	-1.30	-0.10	-0.46	45	6.73	0.43(68-73)+0.32(62-76) +0.30(61-72)
6	36.94	0.492	5.30	0.04	-0.54	28	7.89	0.90(68-70)
7	37.28	0.495	-1.54	-1.16	-4.96	86	3.31	0.75(69-72)-0.45(69-71)
8	40.28	0.002	-0.04	-0.20	-0.21	68	22.88	0.91(69-70)
9	41.53	0.060	-0.49	0.84	1.46	49	17.50	0.68(68-71)+0.40(68-75)
10	41.69	0.099	-0.11	2.12	-0.74	68	18.75	0.34(68-71)-0.34(69-75)
11	43.04	0.006	0.14	-0.03	-0.10	23	11.46	0.71(69-80)
12	43.43	0.037	-0.21	1.00	-0.87	73	20.84	0.55(69-71)+0.49(69-76)
13	45.18	0.007	0.46	-0.22	0.23	38	16.45	0.70(69-73)
14	45.83	0.074	-1.82	-0.06	0.33	28	10.40	0.55(68-78)
15	46.50	0.063	1.66	0.34	0.09	41	9.59	0.39(68-72)
16	46.66	0.484	4.68	-0.39	-0.11	25	11.59	0.59(67-71)
17	47.12	0.022	-0.84	-0.43	0.34	51	9.62	0.40(68-77)
18	47.19	0.015	0.59	0.46	-0.36	61	20.75	0.53(69-75)
19	47.48	0.198	-2.61	1.39	-0.37	21	11.83	0.55(68-78)+0.49(67-71)
20	47.85	0.015	-0.57	-0.53	0.20	66	10.09	0.43(69-78)

^aEn. = Energy in [10³ cm⁻¹]. ^bThe angle between the *S*₀-*S*₁ and *S*₀-*S*_{*n*} transition moment directions. ^cDM = Dipole moment. ^dSee Fig. 5 for the form of molecular orbitals.

TABLE II

Triplet transitions of DFOD calculated by INDO/S. See caption to Table I.

	Energy [10 ³ cm ⁻¹]	Dipole moment [D]	Leading configurations ^a
1	27.48	7.73	0.77(69-73)
2	28.84	6.98	0.89(68-70)
3	29.94	7.68	0.85(69-74)
4	34.57	6.86	0.50(67-72)+0.45(68-71)
5	35.91	6.74	0.58(68-72)+0.41(67-71)
6	36.03	6.63	0.43(68-72)+0.40(62-75)
7	36.68	7.02	0.57(68-71)-0.38(67-70)
8	37.19	6.71	0.42(67-71)+0.42(64-72)
9	37.27	7.10	0.60(66-74)-0.51(65-74)
10	38.30	6.77	0.44(68-75)-0.35(67-70)

^aDue to different parametrization for singlet and triplet states, the orbital energy ordering is changed in the SCF output for the two manifolds. The occupied orbitals 61, 62, 63, 64, 65 calculated for the singlet states correspond to the orbitals 62, 63, 61, 65, 64 calculated with the triplet parametrization; the unoccupied orbitals 72, 73, 76, 77, 78 obtained for singlets correlate with those labelled 73, 72, 80, 76, 77 for the triplets, respectively (see Fig. 5). The labelling of the other frontier orbitals remains the same.

TABLE III
Singlet transitions of the hydrated form of DFOD calculated by INDO/S. See caption to Table I.

	En. ^a	<i>f</i>	<i>M_x</i>	<i>M_y</i>	<i>M_z</i>	α^b [deg]	DM ^c [D]	Leading configurations
1	32.40	0.011	0.48	-0.71	0.11	0	3.38	0.33(65-80)+0.30(66-80)
2	32.99	0.051	-0.77	1.64	0.12	14	7.10	0.71(73-77)
3	33.61	0.012	0.85	0.22	-0.14	72	6.09	0.50(72-75)
4	34.30	0.003	0.28	0.04	-0.31	79	3.10	0.57(66-79)-0.56(65-79)
5	34.55	0.098	2.45	-0.09	0.05	54	6.48	0.48(72-78)
6	35.92	0.289	4.08	-0.63	0.04	48	6.91	0.63(72-74)
7	38.25	0.438	1.94	0.33	-4.53	87	9.39	0.81(73-76)
8	40.87	0.211	2.91	1.50	-0.51	84	9.81	0.57(73-74)-0.46(72-74) +0.45(73-75)
9	43.23	0.033	0.38	1.21	-0.11	51	13.55	0.50(73-83)
10	43.45	0.123	-2.43	-0.31	0.15	64	12.90	0.55(73-75)
11	43.76	0.073	1.64	0.90	0.18	84	7.60	0.50(72-75)
12	44.27	0.170	-2.34	-1.50	0.64	90	10.65	0.48(73-79)
13	44.54	0.041	-0.96	0.65	0.78	46	10.55	0.51(73-79)-0.51(72-76)
14	45.82	0.162	2.39	-1.11	0.76	32	5.32	0.43(73-74)+0.39(72-77)
15	46.01	0.148	0.11	-2.25	-1.32	48	5.70	0.51(72-77)
16	46.65	0.020	0.85	0.02	-0.41	65	6.47	0.43(72-82)+0.37(72-81)
17	46.98	0.348	-3.02	-2.55	0.40	83	7.08	0.53(71-74)
18	47.21	0.057	-1.56	0.31	0.19	47	5.73	0.37(72-77)
19	47.87	0.139	1.61	-1.84	0.45	8	7.12	0.56(72-84)
20	48.23	0.092	0.02	2.00	0.25	37	8.94	0.39(72-79)

^aEn. = Energy in [10^3 cm^{-1}]. ^bThe angle between the S_0-S_1 and S_0-S_n transition moment directions. ^cDM = Dipole moment. ^dSee Fig. 6 for the form of molecular orbitals.

TABLE IV
Triplet transitions of the hydrated form of DFOD calculated by INDO/S. See caption to Table I.

	Energy [10^3 cm^{-1}]	Dipole moment [D]	Leading configurations ^a
1	28.16	7.52	0.85(73-77)
2	28.56	6.17	0.87(72-74)
3	29.78	7.48	0.84(73-76)
4	34.43	6.04	0.50(72-75)
5	35.79	6.25	0.46(72-75)-0.44(72-78)
6	36.51	6.39	0.45(71-75)
7	36.95	6.28	0.41(70-78)
8	37.47	6.41	0.66(68-76)
9	38.44	6.28	0.68(72-77)
10	39.37	2.68	0.39(66-83)

^aThe occupied orbitals 65, 66, 67, 68, 69 calculated for the singlet states correspond to the orbitals 66, 67, 65, 69, 68 calculated with the triplet parametrization; the unoccupied orbitals 76, 77, 79, 80, 81, 82 obtained for singlets correlate with those labelled 77, 76, 85, 79, 92, 80 for the triplets, respectively (see Fig. 6). The labelling of the other frontier orbitals remains the same.

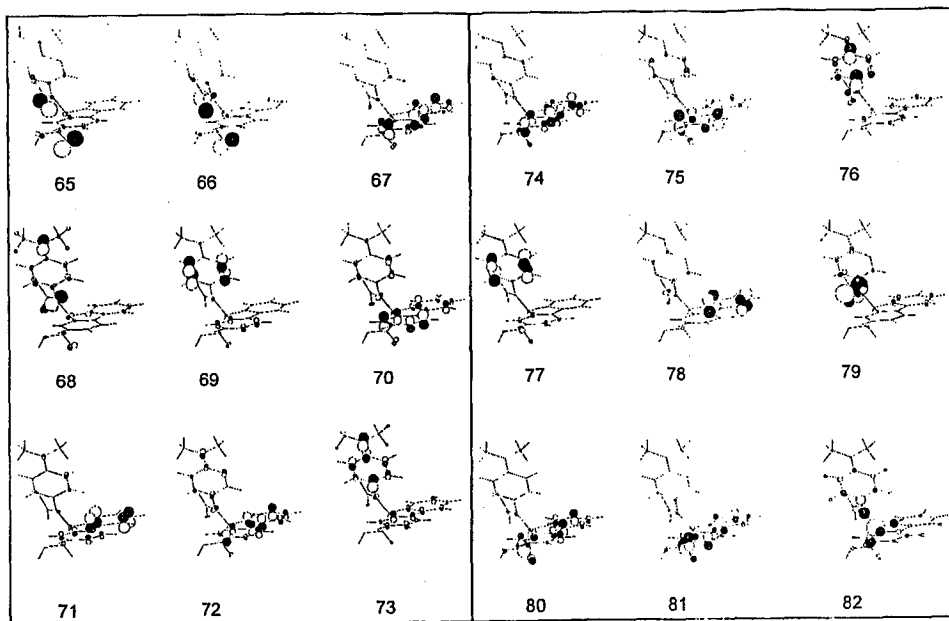


Fig. 6. Highest occupied molecular orbitals (left panel) and lowest unoccupied molecular orbitals (right panel) of the hydrated form of DFOD relevant for the low energy transitions (see Tables III and IV).

where the summation of squares of LCAO coefficients occurs over all atoms of the part *A*. Using this approach, we find very high degree of localization on the fluorene part for orbitals 67, 68 and 70 (0.91, 0.98 and 0.98, respectively), whereas the HOMO orbital (69) is localized on the dimethylaniline ($DL = 0.90$).

Two local strongly allowed transitions calculated at $37\,000\text{ cm}^{-1}$ are predicted to be nearly degenerate. One of them is localized on the fluorene, another on the dimethylaniline part. Yet another strong transition is predicted to lie in the experimentally accessible region, at $46\,660\text{ cm}^{-1}$. For the triplet levels (Table II), the calculations predict the first three states lying within 2500 cm^{-1} . One of them (the second calculated) is localized on fluorene, the other two, on dimethylamine (although the slight delocalization into the fluorene part may be noticed).

The spectral pattern calculated for the hydrated species (Table III) predicts the first excited singlet transition to be blue shifted and stronger than that of DFOD. This is indeed observed (Figs. 1 and 2). Of the two strong transitions which were quasi degenerate in DFOD the one localized on dimethylamine (7th transition in Table I) is expected to shift to the blue while retaining the intensity upon hydration. Again, this is confirmed by absorption as well as linear dichroism experiments in stretched PVA. The orientation factor calculated for the strong peak around $38\,200\text{ cm}^{-1}$ is 0.49 ± 0.02 , which implies that the corresponding transition is polarized approximately parallel to the effective orientation axis. Since

the latter should nearly coincide with the long axis of the dimethylaniline part and be orthogonal to the long axis of the fluorene moiety, the transition is localized on the former.

Similarly to the results for the anhydride, the three lowest triplet states were predicted to lie very close to each other (Table IV).

5. Discussion

Lack of fluorescence in DFOD is not very surprising: both absorption and calculations show that the first excited singlet transition is only very weakly allowed. Somewhat more unusual is the fact that no phosphorescence is observed in the anhydride while it is fairly strong in the hydrated form. One could postulate that the intersystem crossing yield in the latter is much higher than in DFOD, if a higher triplet state comes into the vicinity of S_1 , providing an efficient ISC channel. However, such explanation would imply that the intersystem crossing is dominated by the interaction of only two states, and the phosphorescence should be polarized. The observation that it is not suggests that the spin-orbit coupling involves various singlet transitions of different polarizations (note from Tables I and III that transition moment directions are distributed more or less isotropically in three dimensions). This is not surprising, given the lack of symmetry.

Thus, we are left with an alternative explanation for the lack of phosphorescence of DFOD. The calculations predict three triplet transitions to lie in close vicinity. It is possible that the triplet state localized on the dimethylaniline part is the lowest one in DFOD. Upon hydration, the inversion may occur and the triplet state associated with the fluorene chromophore may become the lowest. The calculations point to such possibility: the two states are computed 1400 cm^{-1} apart in DFOD, while in the hydrate they are expected to be nearly degenerate (Tables II and IV). Comparing the spectral position and shape of phosphorescence with literature data for fluorene [12] and dimethylaniline [12, 13] leaves no doubt that the emission is associated with the fluorene chromophore.

The determination of the triplet character in the two forms may be quite important for the understanding of the photochemistry of DFOD — a desirable task, given that this molecule may find applications as a UV dosimeter. We plan to detect the two different triplet states by ESR spectroscopy, and to combine the electronic spectroscopy and photochemistry studies with IR measurements.

Acknowledgments

We thank M. Cieślak, head of Chemipan, for providing us with the samples of DFOD. Prof. T. Bally is kindly acknowledged for the gift of the MOPLOT program for drawing molecular orbitals.

References

- [1] E.C. Lim, *J. Phys. Chem.* **90**, 6808 (1986).
- [2] J.A. Stikeleather, *Chem. Phys. Lett.* **24**, 253 (1974).
- [3] T. Takemura, H. Baba, *Bull. Chem. Soc. Jap.* **42**, 2756 (1969).
- [4] J. Waluk, A. Grabowska, B. Pakuła, *J. Lumin.* **21**, 277 (1980).

- [5] K. Brenner, J. Lipiński, Z. Ruziewicz, *J. Lumin.* **83**, 13 (1983).
- [6] A. Zweig, W.A. Henderson, Jr., *Photochem. Photobiol.* **24**, 543 (1976).
- [7] J. Jasny, *J. Lumin.* **17**, 149 (1978).
- [8] E.W. Thulstrup, J. Michl, *J. Am. Chem. Soc.* **104**, 5594 (1982); E.W. Thulstrup, J. Michl, *J. Phys. Chem.* **84**, 82 (1980); J. Michl, E.W. Thulstrup, *Acc. Chem. Res.* **20**, 192 (1987).
- [9] PCMODEL, Serena Software, Bloomington, IN, USA.
- [10] J.E. Ridley, M.C. Zerner, *Theor. Chim. Acta* **32**, 111 (1973).
- [11] J.E. Ridley, M.C. Zerner, *Theor. Chim. Acta* **42**, 223 (1976).
- [12] V.L. Ermolaev, *Opt. Spektrosk.* **11**, 492 (1961).
- [13] C. Dubroca, P. Lozano, *Chem. Phys. Lett.* **24**, 49 (1974).